

## Research Article

# Rapid and Sensitive Quantum Dots Immunochromatographic Strip for H10 Subtype Avian Influenza Virus Detection

Jiamin Fu , Ping Wang, Linfang Cheng, Sijing Yan, Han Wu, Xiangyun Lu, Fumin Liu, Hangping Yao, Nanping Wu, and Haibo Wu

State Key Laboratory for Diagnosis and Treatment of Infectious Diseases, National Clinical Research Center for Infectious Diseases, The First Affiliated Hospital, School of Medicine, Zhejiang University, Hangzhou 310003, China

Correspondence should be addressed to Haibo Wu; wuhaibo@zju.edu.cn

Received 27 August 2024; Accepted 26 February 2025

Academic Editor: Linzhu Ren

Copyright © 2025 Jiamin Fu et al. Transboundary and Emerging Diseases published by John Wiley & Sons Ltd. This is an open access article under the terms of the Creative Commons Attribution License, which permits use, distribution and reproduction in any medium, provided the original work is properly cited.

The H10 subtype avian influenza virus (AIV), an important zoonotic pathogen, is widely prevalent in host species (wild fowl) and continues to infect humans, imposing a huge threat to public health. Thus, the H10 subtype AIV is considered a potential pandemic strain and has drawn the attention of scholars worldwide. Therefore, a fast, sensitive, and economical detection method for H10 subtype AIV needs to be developed for the surveillance and prevention of this infection. Quantum dot fluorescent microsphere-based immunochromatographic strip (QDFM-ICS) has a great application prospect in the rapid detection of the virus. In this study, two monoclonal antibodies (1E8 and 2G9) were generated by immunizing mice with the purified hemagglutinin (HA) protein, and QDFM-ICS was designed to detect the H10 subtype influenza antigen. We illustrated that the limit of detection (LOD) of QDFM-ICS for the HA titer and purified HA protein of the H10 subtype AIV was 0.125 per 80  $\mu$ L of the sample and 4 ng/mL, respectively. The specificity of QDFM-ICS was 100%, which indicated that mAb 2G9 specifically bound to the H10 subtype influenza antigen without cross-reacting with other subtype AIVs. The method has good reproducibility. Additionally, the results of preliminary tests on clinical samples showed high consistency between QDFM-ICS and real-time reverse transcription-polymerase chain reaction. The QDFM-ICS has simple analysis steps and can produce objective results within 15 min. Hence, it can be suggested that QDFM-ICS can be used to monitor and prevent the infection caused by H10 subtype AIVs.

**Keywords:** avian influenza virus; fluorescent microsphere; H10 subtype; immunochromatographic strip; monoclonal antibodies; quantum dots

## 1. Introduction

So far, 18 hemagglutinin (HA) and 11 neuraminidase (NA) subtypes of the influenza A virus have been identified based on the antigenicity of surface proteins. Most of these subtypes have been identified in the waterfowl. These subtypes are prevalent as low-pathogenic avian influenza viruses (AIVs) in wild waterfowl worldwide [1]. The H10 subtype AIV was first isolated in 1949 [2] in wild waterfowl [3, 4]. Since then, the H10 subtype has been identified in other wild aquatic birds as well. H10 viruses are known for their ability to continuously adapt to different mammalian species [2, 5]. As a result, they are capable of causing infections in humans. In 2010, Australia reported an

H10N7-associated infection and influenza-like symptoms among its abattoir workers [6]. The first case of avian-origin H10N8 infection in humans, which also resulted in one death, was reported in 2013. In Jiangxi Province, China, at least three cases of H10N8 infections in humans were confirmed, two of which resulted in deaths [7, 8]. In 2021, a new H10N3 subtype influenza A virus was isolated from humans in Jiangsu Province, China. This was also the first documented case of H10N3 infection in humans [9, 10]. The second case of H10N3 infection in humans was reported from Zhejiang Province, China, in 2023 [11]. A death resulting from the H10N5 infection was reported from Zhejiang Province, China [12, 13]. The emergence of AIV

H10 subtype infection in humans emphasizes the persistent and evolving threat posed by AIVs to human health. As AIVs are capable of becoming the next epidemic virus type, they are attracting increasing attention from researchers worldwide [14].

At present, the diagnostic methods available for detecting AIVs include virus isolation [15], nucleic acid-based detection [16–18], and immunoassays, such as enzyme-linked immunosorbent assay (ELISA) [19]. ELISA and reverse transcription–polymerase chain reaction (RT–PCR) are the two most recommended techniques for diagnosing avian influenza [20]. Notably, virus isolation is a highly time-consuming process, while ELISA and PCR require a perfect experimental platform and professional laboratory technicians. Consequently, these methods have limited applications. Moreover, the processing of these methods is cumbersome, and they cannot be used for point-of-care testing [21, 22]. The colloidal gold-based immunochromatographic assay is a popular detection method because it allows rapid, low-cost visualization, without any special equipment. This assay has been used for the detection of influenza virus, infectious bronchitis virus, *Mycoplasma suis*, and other pathogens [23]. However, colloidal gold has some limitations as well, including low sensitivity, an inability to quantify, and a subjective bias [24, 25]. Therefore, it is essential to develop sensitive, efficient, and economic detection methods to prevent and control the outbreaks of AIV [26].

Quantum dots (QDs) have been employed as a new colorimetric label in various immunochromatographic assay systems [27, 28]. QDs have excellent optical properties, including high fluorescence efficiency, broad excitation wave lengths, narrow and symmetric emission spectra, and excellent stability against photobleaching [20, 29, 30]. They have been successfully employed for food safety, biological labeling, and virus detection, such as SARS-CoV-2, influenza A virus, Zika virus, and African swine fever virus [20, 31, 32].

This study aims to produce two specific monoclonal antibodies (mAbs) against the HA of the H10 influenza virus and develop a QD fluorescent microsphere-based immunochromatographic strip (QDFM-ICS) to detect H10-based immunochromatographic strip (QDFM-ICS) to detect H10 subtype AIVs. The specificity of QDFM-ICS was 100%, which indicates that mAb 2G9 did not cross-react with the pathogens of other subtype AIVs. The line of detection (LOD) of QDFM-ICS was 0.125 HA units titer for the H10 subtype AIV per 80  $\mu$ L of the sample. The detection limit of the purified HA protein of H10 AIV was determined to be 4 ng/mL. In addition, we performed preliminary tests using the clinical samples. The results showed high consistency between QDFM-ICS and real-time RT-PCR. The test is easy to perform and can be completed in just 15 min. Hence, QDFM-ICS can be used for point-of-care testing.

## 2. Materials and Methods

**2.1. Cells and Virus.** The Madin–Darby canine kidney (MDCK) cells were obtained from Pricella Biotechnology (Wuhan, China). These cells were cultured and placed in Dulbecco’s modified eagle medium (DMEM, Gibco, Grand Island, New York, United States) supplemented with 10% fetal bovine serum (FBS, Gibco, Auckland, New Zealand). H10 viruses isolated from

chickens in eastern China were used. All the cells and AIVs were stored at  $-80^{\circ}\text{C}$ . We used 9-day-old embryonated chicken eggs to propagate the H10 virus at  $37^{\circ}\text{C}$  and collected the allantoic fluid. We used the collected allantoic fluid and 1% chicken red cells to detect the H10 virus titer. In addition, we performed a tissue culture infectious dose 50 (TCID<sub>50</sub>) assay [33]. The purified HA protein of A/chicken/Zhejiang/2CP8/2014 (H10N7) was generated according to the standard procedure and stored at  $-80^{\circ}\text{C}$  [34], and the GenBank accession number of HA is KP412448. All the viruses used are described in Table 1. All viruses used in the study were stored in our laboratory.

**2.2. Generation and Purification of Murine Monoclonal Antibodies.** All BALB/c mice (6-week-old females) were sourced from SLAC Laboratory Animal Co. Ltd. (Shanghai, China). These mice were housed in a specific pathogen-free environment, where they were kept in a carefully controlled environment at a constant temperature and 60% humidity. The animal experiments conducted using these mice were approved by the Animal Care and Use Committee of the First Affiliated Hospital, Zhejiang University School of Medicine (No. 2022-16).

The purified HA protein extracted from the H10 subtype AIV was mixed with the Quick Antibody-Mouse 5W adjuvant (Biodragon, Suzhou, China) and used to immunize 6-week-old BALB/c mice through intramuscular injection every 2 weeks. After 4 weeks, the antibody titer was measured using the blood samples collected from the tail veins of the mice. Next, HA protein without the adjuvant was injected into the mouse exhibiting the highest antibody titer to further immunize it. 3 days later, lymphocytes were collected from the spleen of this mouse and fused with SP2/0 cells. Additionally, we collected supernatants from the hybridoma cell culture to detect their reactivity with the purified HA protein by conducting ELISA using H10-coated HA protein. This process helped identify and obtain monoclonal hybridoma cell lines exhibiting the desired reactivity. The mice were then inoculated with these monoclonal hybridoma cell lines. Finally, we obtained purified mAbs from the ascites of these mice by using a Protein G column (GE Healthcare, Chicago, IL, USA).

**2.3. Isotypes and Affinity of mAbs.** A moderate amount of purified mAbs was added to the monoclonal antibody isotyping kit (Bio-Rad, USA) to identify the isotypes. Pipetting the mAbs sample into the development tube where it forms a complex with the antibody coated micro particles and inserting the strip. This complex flows through the strip until it is bound by the immobilized goat antimouse antibody specific for the monoclonal’s isotype and its light chain. In  $\sim 5$ –10 min, the micro particle complex will aggregate as blue bands in the two sections corresponding to the monoclonal antibody’s isotype and its light chain. The affinities of all mAbs were investigated using the methodology outlined was described previously [35]. Briefly, the purified mAbs (Section 2.1) were first diluted to 20 ng per well using an ELISA coating buffer (KPL, Milford, MA, USA) and then added to the ELISA plate overnight at  $4^{\circ}\text{C}$ . The next day, the plate was washed five times with PBS and then blocked with a blocking buffer (KPL) for 2 h. The plate was again washed five times with PBS, and mAbs

TABLE 1: Respiratory viruses mentioned in the research.

Virus strains	QDFM- ICS	Reference real-time RT-PCR
A/duck/Zhejiang/D1/2013(H1N2)	—	+
A/duck/Zhejiang/6D10/2013(H2N8)	—	+
A/duck/Zhejiang/4613/2013(H3N2)	—	+
A/duck/Zhejiang/409/2013(H4N6)	—	+
A/duck/Zhejiang/6D2/2013 (H5N6)	—	+
A/chicken/Zhejiang/1664/2017(H6N1)	—	+
A/chicken/Zhejiang/DTID-ZJU01/2013(H7N9)	—	+
A/chicken/Zhejiang/329/2011(H9N2)	—	+
A/duck/Zhejiang/6D20/2013(H10N2)	+	+
A/chicken/Zhejiang/8615/2016(H10N3)	+	+
A/Zhejiang/CNIC-ZJU01/2023(H10N5)	+	+
A/chicken/Zhejiang/2CP8/2014(H10N7)	+	+
A/chicken/Zhejiang/102615/2016(H10N8)	+	+
A/duck/Zhejiang/71750/2013(H11N9)	—	+
Infectious bronchitis virus (IBV, H120)	—	ND
Newcastle disease virus (NDV, La Sota)	—	ND
Infectious bursal disease virus (IBDV, NF8)	—	ND
Avian paramyxovirus-4 (APMV-4, ZJ-1)	—	ND

Abbreviations: ND, not detected; QDFM-ICS, quantum dot fluorescent microsphere-based immunochromatographic strip; RT-PCR, reverse transcription-polymerase chain reaction.

(Section 2.2) was added to it by conducting multiple dilutions for 1 h at 37°C. The plate was again washed three times with PBS and incubated with PBS-diluted secondary antibodies at 37°C for 30 min. Finally, the absorbance of all samples on the ELISA plate was measured using an ELISA reader.

**2.4. Immunofluorescence.** An immunofluorescence assay was conducted to assess the specific binding between different subtypes of AIV (H10N2, H10N3, H10N5, H10N7, H10N8, H1N2, H3N2, H6N1, H7N9, and H9N2) and mAbs 2G9 and 1E8 [36]. MDCK cells were first treated with different subtypes of AIV and then washed with PBS and fixed with pro-cooled methanol. Next, the MDCK cells were permeabilized with 0.3% Triton X-100 and washed three times with PBS. Additionally, the cells were blocked with a blocking buffer for 1 h and then incubated overnight with mAb 2G9 and 1E8. Following the initial washing of the cells with PBS, the cells were incubated with goat antimouse IgG heavy plus light chain (H + L)-Alexa Fluor 488 (Abcam, England) for 90 min. After this incubation, the cells were again washed with PBS three times. The images were captured using a Leica sp8 confocal laser scanning microscope (Leica, Germany).

**2.5. Hemagglutination Inhibition (HI) and Virus Neutralization (VN) Tests.** The experimental steps of hemagglutination inhibition (HI) were carried out according to the methodology outlined in a previous study [33]. The H10N7 virus was prepared by diluting it to a concentration of 8 HA units (HAU) in PBS and was set aside for use. Twofold serial dilutions of H10 mAbs were prepared, with concentrations ranging from 10 to 0.01 µg/mL. These dilutions were then introduced into a microtiter plate; 25 µL of each dilution was added to every well. Then, an equal amount of H10 was added to each well. A negative

control with PBS was prepared. The mixture was incubated for 40 min at room temperature. Finally, 50 µL of 1% chicken red blood cells was added to each well and reacted with the unbinding HA to determine the HI titer. The results were observed after 20 min. The virtual neutralization (VN) test was performed as follows [37]. Twofold serial dilutions of H10 mAbs, which ranged from 100 to 0.2 µg/mL, were added into a microtiter plate. An equal amount of 100 TCID<sub>50</sub> of the H10N7 virus was added to each well for 2 h. The MDCK cells were washed with phosphate-buffered saline (PBS) and supplemented with the mixture described above for 72 h. The supernatant was collected, and the presence of virus was detected through a HA assay. The Reed–Muench method was used to calculate the neutralization titers [38].

**2.6. Generation of Antibody Escape Mutants.** Equal volumes of H10 mAb and 100TCID<sub>50</sub> of H10 virus (10 µg/mL each) were mixed and incubated for 1 h at room temperature. Following this incubation period, 200 µL of the mixture of mAb and H10 virus was administered into 9-day-old embryonated chicken eggs. These eggs were incubated for 72 h at 35°C. After the incubation, the allantoic fluid was harvested and subsequently tested to determine the HA titer. The positive allantoic fluid was collected and mixed with increasing mAbs concentrations, ranging from 10 to 160 µg/mL. The above steps were carried out five times. RNA was extracted using the Trizol LS reagent (Life Technologies, Waltham, MA, USA). The HA segment was amplified by RT-PCR, and the amino acid changes were detected by sequencing as described in a previous study [39]).

**2.7. Establishment of QDFM-ICS.** First, 30 µL of QDs was dissolved in 400 µL of 25 mM 4-morpholineethanesulfonic

acid (MES, Sigma–Aldrich, Saint Louis, MO, USA) adjusted to pH 6.0. The resulting mixture was supplemented with 15  $\mu$ L of 1-ethyl-3-(3-dimethylaminopropyl) carbodiimide hydrochloride (EDC, Thermo Fisher Scientific, Rochford, USA) at 10 mg/mL and 15  $\mu$ L of N-hydroxysuccinimide (NHS, Sigma–Aldrich) at 10 mg/mL [30]. The mixture was gently shaken horizontally for 30 min at room temperature to fully activate the carboxyl. The redundant EDC and NHS were removed by performing centrifugation (15000 rpm) for 30 min at 4°C [32]. The QDs were resuspended in 400  $\mu$ L of MES with 0.2 mg of mAb 2G9. The mixture was incubated to allow the binding of mAb with QDs for 1 hr at room temperature, as shown in Figure 1A. Additionally, 400  $\mu$ L of the blocking buffer supplemented with 2% bovine serum albumin (BSA, Sangon Biotechnology, Shanghai, China) was employed to block the unbound sites and incubated for another hour. The washing buffer was used to remove the unbound antibodies or chemicals [20]. The activated QDs were resuspended in 150  $\mu$ L of MES (containing 2% BSA) and were sprayed evenly onto glass cellulose membranes (Jiening Biotechnology, Shanghai, China). The goat antimouse IgG (Solarbio, Beijing, China) at a concentration of 1 mg/mL and mAb 1E8 at a concentration of 4 mg/mL were dispensed onto the NC membrane by using a BioDot XYZ distribution platform (Jinbiao Biotechnology, Shanghai, China) with a dispensing parameter of 1  $\mu$ L/cm to generate the C, T lines. The QDFM–ICS, comprising a sample pad, glass cellulose membranes, nitrocellulose (NC) membranes (Sartorius, Göttingen, Germany), and an absorbent pad (Jiening Biotechnology), was assembled on a polyvinyl chloride (PVC) backplate (Jiening Biotechnology), as shown in Figure 1B. The assembled PVC backplate was cut into 3.5-mm-wide strips using an automatic cutting machine (Jinbiao Biotechnology). The strips were observed under 365-nm UV light with the naked eye. The fluorescence intensity was measured using a fluorescence test strip scanner (Hemai Technology, Suzhou, China).

**2.8. Specificity, Sensitivity, and Reproducibility of the H10 QDFM–ICS.** The specificity of the QDFM–ICS was evaluated as follows. Different subtypes of AIVs (H10N2, H10N3, H10N5, H10N7, H10N8, H1N2, H2N8, H3N2, H4N6, H5N6, H6N1, H7N9, H9N2, and H11N9) and other avian viruses, avian paramyxovirus-4 (APMV-4, ZJ-1), infectious bronchitis virus (IBV, H120), infectious bursal disease virus (IBDV, NF8), and Newcastle disease virus (NDV, La Sota) were added to the aforementioned strips to detect the specificity of the QDFM–ICS through naked eye observation. The absorbance was also detected. The allantoic fluid containing  $2^6$ – $2^6$  HAU of the H10 AIV and 2000–0.5 ng/mL of purified H10 HA proteins, which were twofold serial diluted, was added to the strips to detect the sensitivity of QDFM–ICS. To evaluate the reproducibility, the H10 AIV allantoic fluid, which was diluted to  $2^4$ ,  $2^1$ , and  $2^{-2}$  HAU, was used 20 times, and the relative standard deviation (RSD) value was calculated using the absorbance value.

**2.9. Poultry Sample Test.** To evaluate the effectiveness of the QDFM–ICS established, 160 samples, including 25 H10 positive samples (5 avian cloacal swabs, 2 avian throat swabs, and

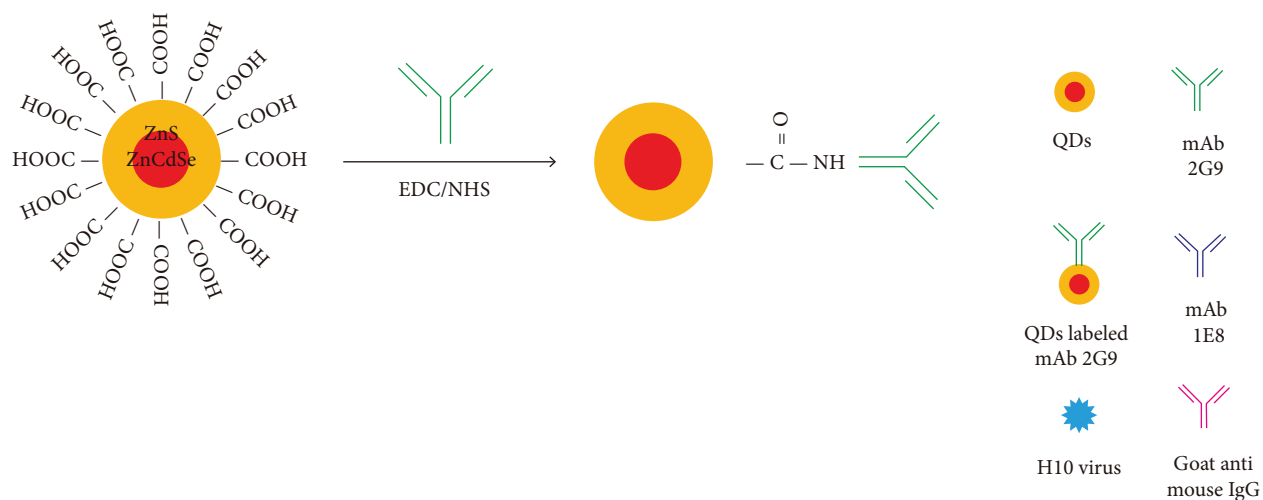
18 fecal samples) [55], were investigated using real-time RT–PCR and QDFM–ICS methods. An influenza A virus real-time RT-PCR kit (Liferiver, Shanghai, China) was performed according to the manufacturer’s instructions and used as the reference method [40]. The data so obtained were analyzed using the CFX96 System (Bio-Rad, CA, USA).

### 3. Results

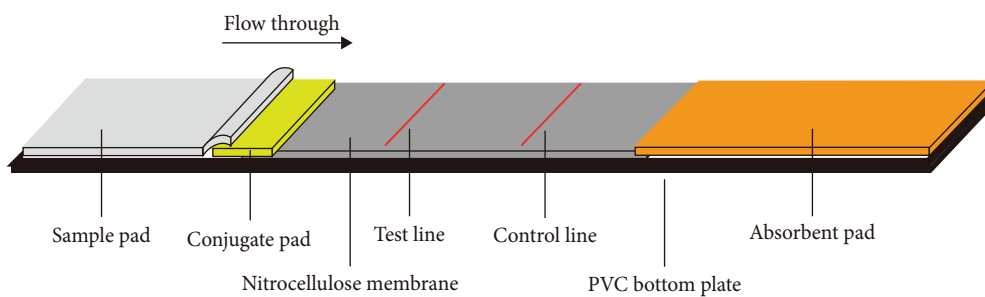
**3.1. Generation and Characterization of mAbs.** First, we immunized the mice with the purified HA of the H10N7 virus and fused their spleen cells with myeloma cells to create hybridomas. We conducted an ELISA assay to identify the hybridoma cell lines that could stably secrete HA-specific mAbs. For this assay, we used the immunizing antigen as the coating to screen and select the appropriate hybridoma line [41]. Two cell lines, 1E8 and 2G9, were chosen for further investigations. The isotypes of these mAbs, IgG2b for 1E8 and IgG2a for 2G9, and the sequence characterization of their heavy and light chains are listed in Table 2. Both mAbs demonstrated a strong binding affinity for the HA of the H10N7 virus. The immunofluorescence results confirmed their binding specificity (Figure 2). None of the two mAbs demonstrated any nonspecific binding when tested on MDCK cells infected with H1N2, H3N2, H6N2, H7N9, and H9N2 subtype AIVs. Conversely, both 1E8 and 2G9 displayed robust reactivity toward MDCK cells infected with H10 viruses. This obvious reactivity underscores the high specificity of these mAbs for the H10 viruses.

**3.2. Amino Acid Substitutions Selected by mAbs.** We initiated a series of assessments to investigate the amino acid substitutions. We cultured H10N7 viruses (A/chicken/Zhejiang/2CP8/2014) in the presence of mAbs at concentrations of 10, 20, and 40  $\mu$ g/mL to generate escape mutants and pinpoint the specific mAb epitopes. After four passages, the escape viruses were gathered and the nucleotide sequences of their HA genes were analyzed through sequencing. These sequences were then compared to those of the parent strains to assess any genetic changes. Our results indicated that in the H10N7 virus, mutants escaping from 1E8 exhibited the K165E mutation, while those from 2G9 showed the N170D mutation, both located in the 150-loop region (H3 numbering) of the HA protein (Figure 3). A total of 1833 HA genes in H10 were obtained from the GISAID and aligned using the MEGA11 software. The results show that K165 and N170 are highly conserved. In circulating H10 strains, the probability of K165E and N170D mutations occurring is very low, at 0.22% and 0.11%, respectively.

**3.3. LOD of QDFM–ICS.** To explore the performance of the QDFM–ICS in detecting the A/chicken/Zhejiang/2CP8/2014 (H10N7) influenza virus, we conducted tests using three replicate samples containing  $2^{-6}$ – $2^6$  HAU of H10N7. As shown in Figure 4, the fluorescence intensity observed on the test line is directly related to the virus concentration. Notably, the fluorescence from the H10N7 test line at  $2^{-2}$  HAU can be observed by the naked eye (Figure 4A). However, the fluorescence test strip scanner was allowed to detect only a low titer of H10N7 ( $2^{-3}$



(A)



(B)

FIGURE 1: Continued.

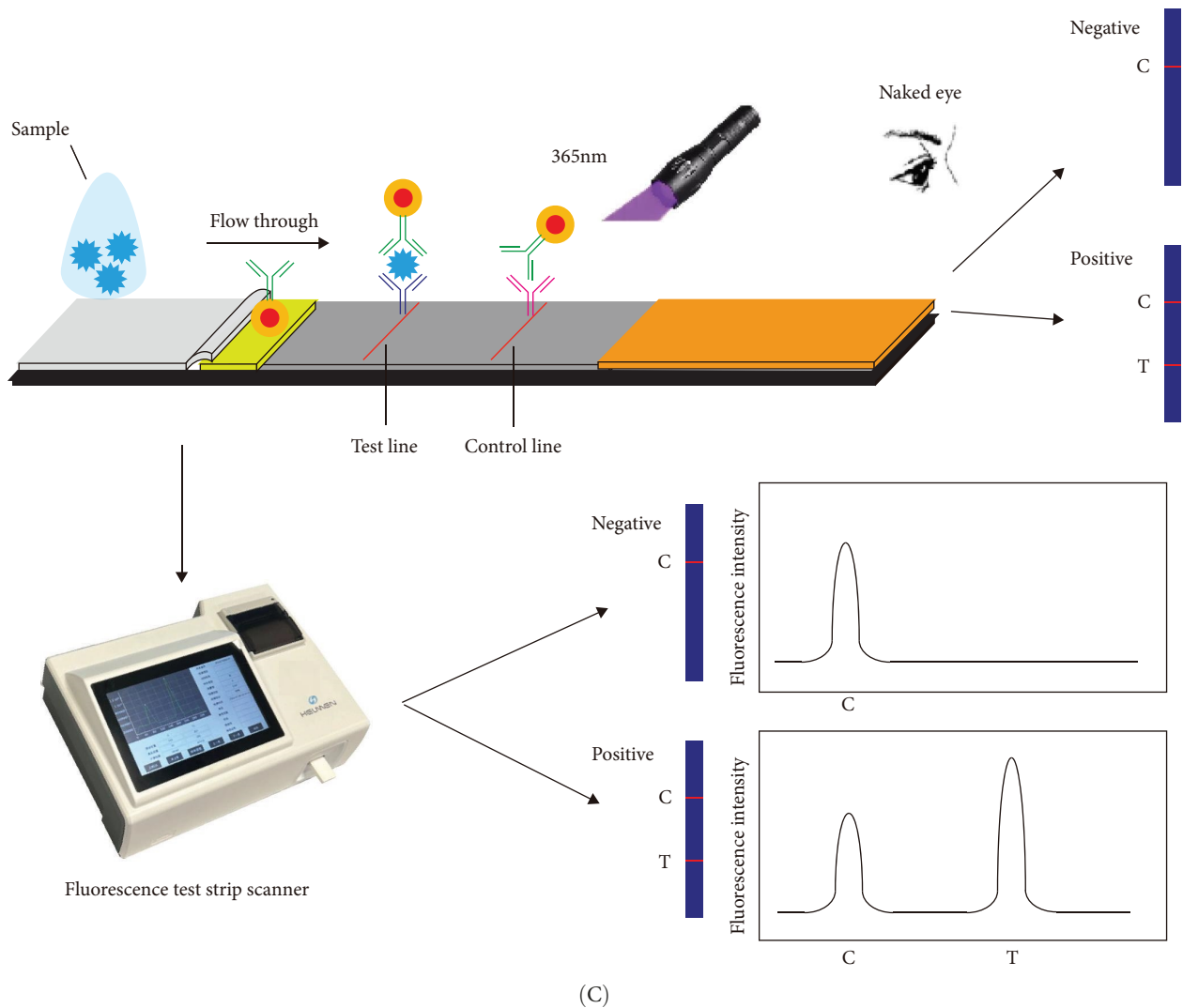


FIGURE 1: Schematic representation of QDFM-ICS. QDFM-ICS, quantum dot fluorescent microsphere-based immunochromatographic strip.

HAU) (Figure 4B). Additionally, the fluorescence from the test line containing 4 ng/mL of the purified H10N7 HA protein can be observed unaided (Figure 4C). The fluorescence test strip scanner could detect the purified H10N7 HA protein at a concentration of 4 ng/mL (Figure 4D). The fluorescence intensity of this protein is  $\sim 800$ .

**3.4. Specificity of QDFM-ICS.** We examined non-H10 subtypes of influenza viruses (including H1N2, H2N8, H3N2, H4N6, H5N6, H6N1, H7N9, H9N2, and H11N9) as well as other avian respiratory tract virus strains, including common NDV, IBV, IBDV, and APMV-4. The results showed that QDFM-ICS only reacts with the H10 subtypes of AIV (including H10N2, H10N3, H10N5, H10N7, and H10N8), without showing any cross-reactivity with other influenza A virus subtypes or other viruses tested (Figure 5). This lack of interference ensures that accurate and reliable results are obtained for diagnosing the intended target virus. Hence, it is evident that the QDFM-ICS exhibits high specificity for detecting H10 AIVs.

**3.5. Reproducibility of QDFM-ICS.** The reproducibility of the QDFM-ICS was evaluated by detecting absorbance from 20 replicates across different titers of the H10 virus ( $2^4$ ,  $2^1$ , and  $2^{-2}$  HAU). As illustrated in Table 3, the RSD values were consistently below 10%, which demonstrates the robust reproducibility of the QDFM-ICS method. The signals produced by 20 replicates of different concentrations of the H10 virus ( $2^4$ ,  $2^1$ , and  $2^{-2}$  HAU) were detected to test the reproducibility of this QDFM-ICS. As demonstrated in Table 3, all the RSD values are below 10%, which indicates that the QDFM-ICS exhibits a high degree of reproducibility. Low RSD values are indicative of the consistent performance and reliability of the assay.

**3.6. Actual Application of QDFM-ICS Sample Tests.** We analyzed 160 avian samples using QDFM-ICS, among which 25 were confirmed as H10 positive (comprising 5 cloacal swabs, 2 throat swabs, and 18 fecal samples). The accuracy of the QDFM-ICS method was thoroughly assessed by comparing its results to those obtained from a real-time RT-PCR assay

TABLE 2: Characterization of mAbs to H10N7 virus.

Name	HI titer <sup>a</sup>	MN titer <sup>a</sup>	Affinity (µg/mL) <sup>b</sup>	Isotype <sup>c</sup>		Heavy chain		Light chain	
				Subclass	Type	V-GENE and allele	CDR3 <sup>d</sup>	V-GENE and allele	CDR3
1E8	8	2	$4 \times 10^{-4}$	IgG2b	k	Musmus IGHV8-12*02 F	ARSPPTDYGSSWGVMDY	Musmus IGKV4-59*01 F	QQWSSNPLT
2G9	8	8	$2 \times 10^{-4}$	IgG2a	k	Musmus IGHV9-3-1*01 F	ARGYDYAEGYFAMDY	Musmus IGKV8-30*01 F	QQYYSNYNT

Abbreviation: ELISA, enzyme-linked immunosorbent assay.

<sup>a</sup>HI and MN titers of these mAbs were measured against A/chicken/Zhejiang/2CP8/2014(H10N7). The initial concentration of these Abs was 20 µg/mL for HI and 100 µg/mL for MN.

<sup>b</sup>The ELISA was performed using the HA protein of A/chicken/Zhejiang/2CP8/2014(H10N7).

<sup>c</sup>The isotyping of the mAbs was performed using a Mouse Monoclonal Antibody Isotyping Test Kit.

<sup>d</sup>Complementarity-determining region.

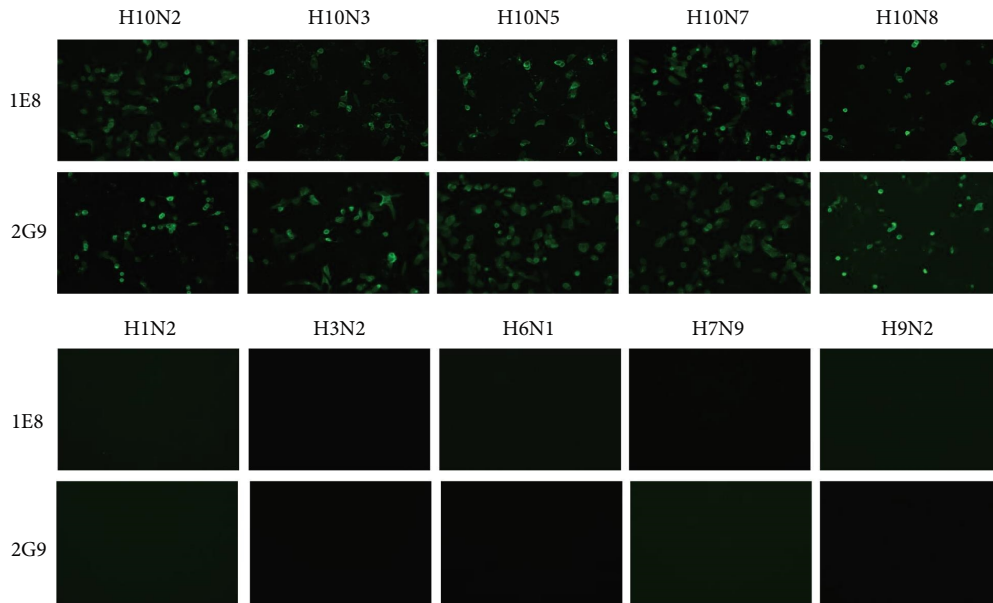


FIGURE 2: Immunofluorescence assay to measure the binding specificity of mAbs to different subtypes influenza virus. MDCK cells infected with H10N2 (A/duck/Zhejiang/6D20/2013), H10N3 (A/chicken/Zhejiang/8615/2016), H10N5 (A/Zhejiang/CNIC-JU01/2023), H10N7 (A/chicken/Zhejiang/2CP8/2014), H10N8 (A/chicken/Zhejiang/121711/2016), H1N2 (A/duck/Zhejiang/D1/2013), H3N2 (A/duck/Zhejiang/4613/2013), H6N1 (A/chicken/Zhejiang/1664/2017), H7N9 (A/chicken/Zhejiang/DTID-ZJU01/2013), and H9N2 (A/chicken/Zhejiang/329/2011) influenza viruses were incubated with mAbs (1E8 and 2G9). Binding by mAbs was detected by Alexa Fluor 488 (green) conjugated secondary antibodies.

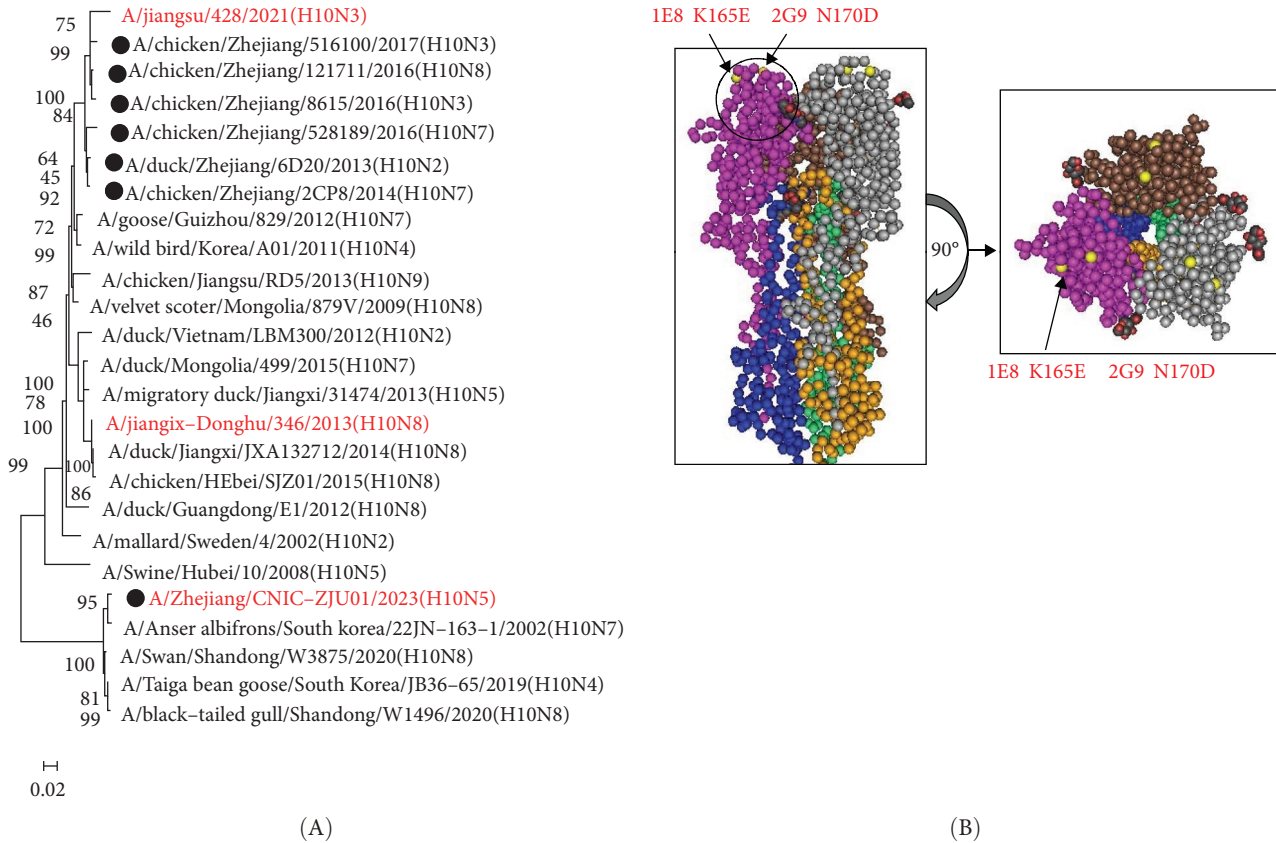
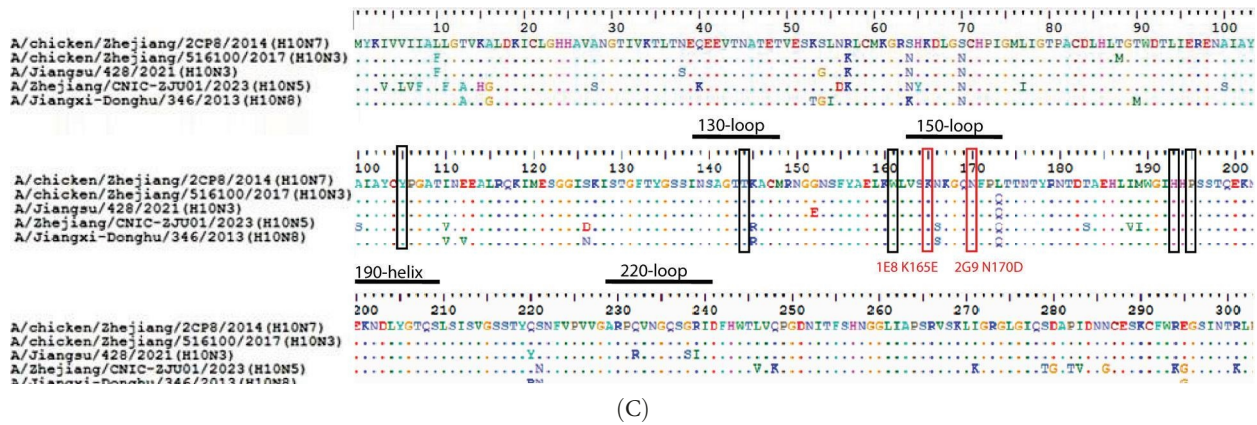


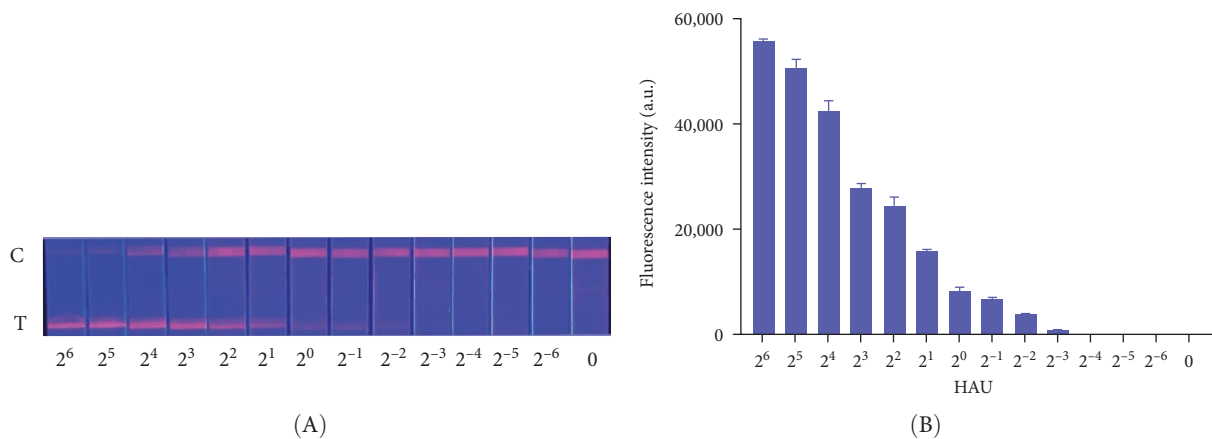
FIGURE 3: Continued.



Name	Mutation	Residues observed in circulating H10 strains
1E8	K165E	K (99.40%, 1822/1833), G (0.27%, 5/1833), E (0.22%, 4/1833), N (0.05%, 1/1833), R (0.05%, 1/1833)
2G9	N170D	N (99.45%, 1823/1833), T (0.22%, 4/1833), S (0.16%, 3/1833), D (0.11%, 2/1833), K (0.05%, 1/1833)

(D)

FIGURE 3: Phylogenetic analysis and mutation site analysis of H10 AIVs. (A) A phylogenetic analysis of the HA genes of representative H10 influenza viruses. The evolutionary tree was created by the neighbor-Joining method and bootstrapped with 1,000 replicates using MEGA11. The influenza viruses used in this study are highlighted by dots, and the H10 influenza viruses that caused human infection in China indicated in the red. (B) Escape mutations detected in this study were displayed in the crystal structure of A/Jiangxi-Donghu/346/2013 (H10N8) (Protein Data Bank code: 4QY0). The mAbs (1E8 and 2G9) escape mutations are indicated in yellow. The circle represents the receptor pocket of HA protein. (C) Sequence alignments of the HA protein of H10 influenza virus and escape mutations of mAbs, located in the 150-loop region (H3 numbering) of the HA protein. The receptor pocket is formed by 4 secondary structural elements, the 130-, 150-, and 220-loops and the 190-helix. Five conserved residues, Y98, T136, W153, H183, and P185 (H3 numbering), form the base of the pocket, indicated in black boxes. (D) Conservation of H10 HA residues substituted in mAb resistant mutants. A total of 1833 H10 HA protein sequences from the GISAID were analyzed. In circulating H10 strains, the K165E substituted was observed in four strains: A/duck/Manitoba/1953 (H10N7), A/duck/Hubei/137/1985 (H10N4), A/duck/Hong\_Kong/934/1980 (H10N5), and A/ruddy\_turnstone/King\_Island/14063/2019 (H10N5); while the N170D substituted was observed in two strains: A/duck/Hokkaido/18/2000 (H10N4) and A/chicken/Zhejiang/HY25/2021 (H10N3).



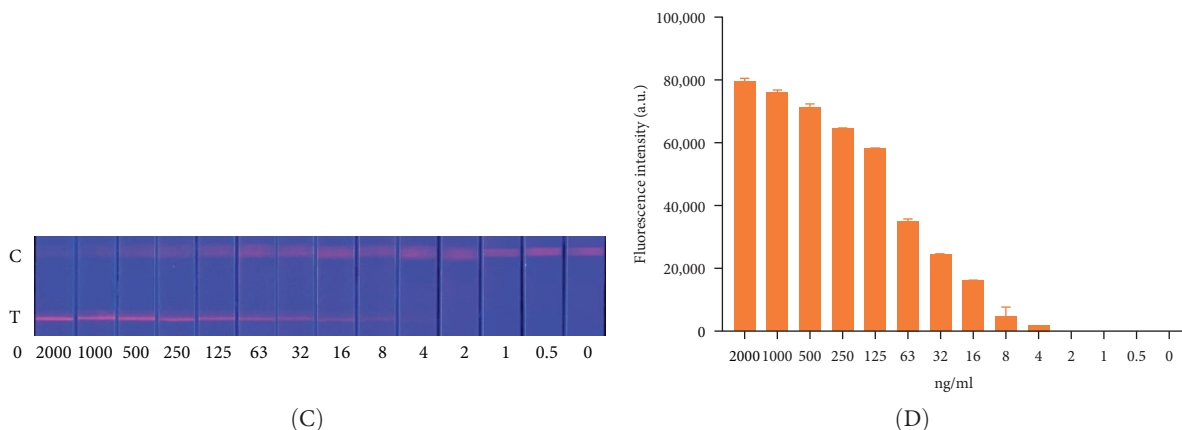


FIGURE 4: Images of tested QDFM-CIS in response to excitation with 365-nm ultraviolet light. (A) Serial dilutions of H10N7 AIV ranging from  $2^{-6}$  to  $2^6$  HAU were used to determine the limit of detection of the QDFM-ICS. (B) Fluorescence intensity scans at different concentrations of H10N7 measured by the fluorescence test strip scanner. (C) Serial dilutions of purified H10N7 HA protein ranging from 2000 to 0.25 ng/mL were used to determine the limit of detection of the QDFM-ICS. (D) Fluorescence intensity scans at different concentrations of purified H10N7 HA protein measured by the fluorescence test strip scanner. QDFM-ICS, quantum dot fluorescent microsphere-based immunochromatographic strip.

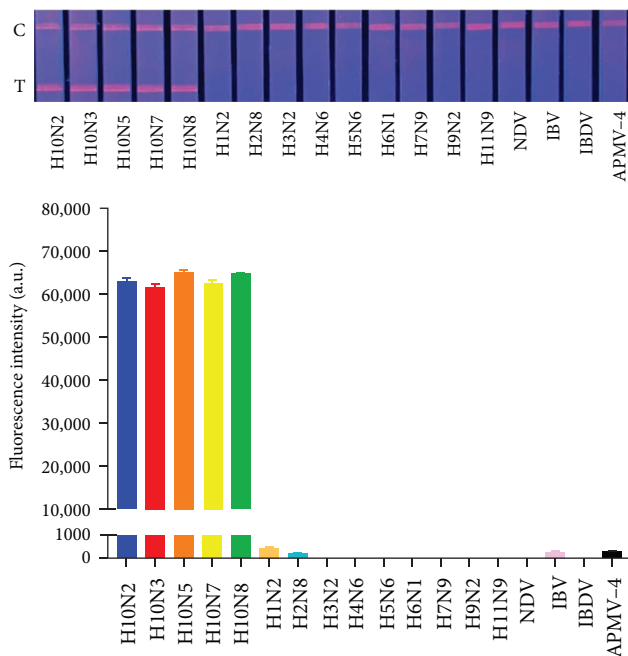


FIGURE 5: Cross-reactivity tests of influenza A viruses (including H10N2, H10N3, H10N5, H10N7, H10N8, H1N2, H2N8, H3N2, H4N6, H5N6, H6N1, H7N9, H9N2, and H11N9) and other avian respiratory tract viruses (including NDV, IBV, IBDV, and APMV-4).

—the reference method for evaluation. This comparison helped in determining how well the QDFM-ICS method performed in relation to the established real-time RT-PCR technique. As detailed in Table 4, both methods yielded identical results, demonstrating 100% concordance. Hence, it can be suggested that QDFM-ICS performs reliably well across diverse sample types without interference, with high sensitivity and specificity.

#### 4. Discussion

H10 subtype AIVs have been reported in a wide variety of species worldwide, including poultry [6], harbor seals [42], and humans [9, 43]. In Eastern and Southern China especially, multiple novel reassortant H10 subtype AIVs have been identified, such as H10N3 [44], H10N7 [45], H10N8 [46], and H10N9 [47]. Continuous mutations and recombination have enabled these H10 subtype AIVs to breach the species barrier, enabling their transmission to humans. Human cases of H10 subtype AIV infection continue to emerge, which have also resulted in deaths. For example, in China, H10N8 [7] and H10N5 [12] infections have resulted in one death each. Hence, it is crucial to rapidly and accurately detect these viruses for effective disease surveillance and prevention. It is essential to remain vigilant and develop rapid response measures to mitigate risks to public health owing to any potential outbreaks [48, 49]. Ensuring timely and precise detection is crucial for monitoring the spread of these viruses and implementing appropriate measures to control and prevent their outbreaks.

At present, ELISA and colloidal gold immunochromatographic test (ICT) strip are the chief antibody-based virus detection methods. These detection methods allow swift identification of influenza viruses. For instance, an ELISA and a colloidal gold ICT strip, both of which utilize mAbs, have been specifically developed for detecting the H9N2 subtype AIV. The ELISA has a detection limit of 4 HAU and 31.5 ng/mL of the HA protein, which indicates its sensitive and precise detection capabilities [35]. We developed an H7N9 mAb-based colloidal gold ICT strip to detect the H7N9 AIV. The LOD of this method for the H7N9 virus was 2 HAU [41]. He et al. developed an innovative dual-function-ELISA for the universal diagnosis of H7 subtype AIVs. This versatile ELISA can detect either the antigen or the antibody associated with the virus. Notably, the assay is highly sensitive, with an antigen detection limit of less than 1 HAU for H7 subtype AIVs, making it a

TABLE 3: Reproducibility QDFM-ICS.

Virus concentrations (HAU)	Fluorescence intensity average (a.u.)	Std. dev	RSD/% (n = 20)
2 <sup>4</sup>	53,115	5142.0	9.68
2 <sup>1</sup>	9343	857.2	9.17
2 <sup>-2</sup>	3767	279.2	7.41

Abbreviations: HA, HA units; QDFM-ICS, quantum dot fluorescent microsphere-based immunochromatographic strip; RSD, relative standard deviation.

TABLE 4: Sample tests using QDFM-ICS or real-time PCR.

Samples	Number	QDFM-ICS result (P/N)	Real-time PCR result (P/N)
Cloacal swab	20	5/20	5/20
Throat swab	30	2/30	2/30
Fecal samples	110	18/110	18/110

Abbreviations: PCR, polymerase chain reaction; QDFM-ICS, quantum dot fluorescent microsphere-based immunochromatographic strip.

highly suitable method for accurately identifying H7 infections [50]. Notably, the LODs of these methods are subject to further improvement.

The QD-based detection method is another rapid, sensitive, and economical antibody-detection method. This method exhibits significant application potential for the rapid detection of viruses. A QD-based lateral flow immunoassay system for simultaneous detection of the H5 and H9 subtypes of AIV has been reported. This advanced system demonstrated impressive sensitivity, with the detection limits of 0.016 HAU for the H5 AIV and 0.25 HAU for the H9 AIV. The use of QDs in this lateral flow immunoassay enhances its ability to accurately identify both the H5 and H9 subtypes at remarkably low concentrations [22]. A QD-based fluorescent immunochromatographic assay specifically for detecting SARS-CoV-2 has also been reported. This advanced method can identify the virus within just 15 min, with an impressive detection limit (5 pg/mL) for the virus antigen. A QD-microsphere-based test strip for detecting the African swine fever virus, with a detection limit of 1 copy, has also been reported [20, 51]. Adegoke et al. [31] developed a plasmonic nanoparticle-QD-molecular beacon biosensor probe for detecting the RNA of the Zika virus, with a detection limit of less than 3 copies/mL [31]. Our findings reveal that the LOD of QDFM-ICS for H10 subtype AIV could reach 0.125 HAU. This detection capability was notably superior to that of the colloidal gold-based immunochromatographic assay. Consequently, the QDFM-ICS method demonstrates a significantly higher sensitivity and can have a broader and more effective application in practical settings.

This study also analyzed 1E8 K165E and 2G9 N170D, the escape mutation sites. Both of these sites are located in the receptor-binding region and are the molecular basis of H10 AIV infection in humans. Notably, virus evolution and mutation put these sites under great immune pressure, which may further increase the frequency of mutation [52, 53]. Analysis of these escape mutation sites can not only clarify the antigenicity of the virus but can also help in the study of the influenza

vaccine. If these mAbs are capable of neutralizing the virus, they can be employed in antiviral drug development studies. In addition, the analysis of virus antigen sites can enable timely monitoring of the applicability of the method to epidemic strains. The risk of missed detection increases if a mutation occurs in the interaction sites between the antigen and the antibody. It is necessary to reduce the time required for antibody detection, in order to improve the applicability of the detection method. Therefore, the analysis of virus antigen sites is of great significance for virus detection.

## 5. Conclusions

A sensitive QDFM-ICS was designed to detect the H10 subtype influenza virus. The QDFM-ICS uses a simple 365-nm fluorescence device. It can rapidly analyze the samples and afford reliable results within 15 min. The LOD of QDFM-ICS in detecting H10 subtype AIV was 0.125 HAU per 80  $\mu$ L of the sample, with a corresponding LOD of 4 ng/mL for the HA protein of H10 AIV. Furthermore, the QDFM-ICS method demonstrated both high specificity and excellent reproducibility, ensuring reliable and accurate results. The tests on clinical samples showed high consistency between the QDFM-ICS and real-time RT-PCR results. The QDFM-ICS allows fast and accurate point-of-care testing along with an acceptable performance. Hence, QDFM-ICS is a promising method for virus detection and affords new options for point-of-care testing.

## Data Availability Statement

All data of this study are available from the corresponding author upon request.

## Ethics Statement

The Animal Ethics Committee of First Affiliated Hospital, School of Medicine, Zhejiang University approved all animal experiment in this study (No. 2022-16).

## Conflicts of Interest

The authors declare no conflicts of interest.

## Author Contributions

Jiamin Fu and Ping Wang have contributed equally to the work.

## Funding

This work was supported by Grants from the National Science Foundation of the People's Republic of China (32273092), Zhejiang Provincial Natural Science Foundation of China (LY24H190001), and National Key R&D Program of China (2024YFC2309903).

## References

- [1] R. Xie, K. M. Edwards, M. Wille, et al., "The Episodic Resurgence of Highly Pathogenic Avian Influenza H5 Virus," *Nature* 622, no. 7984 (2023): 810–817.
- [2] Z. Yuan, J. Zhang, D. Jiang, G. Huang, and W. Qi, "Epidemiology and Evolution of Human-Origin H10N5 Influenza Virus," *One Health* 19 (2024): 100893.
- [3] H. Feldmann, E. Kretzschmar, B. Klingeborn, R. Rottj, H.-D. Klenk, and W. Garten, "The Structure of Serotype H10 Hemagglutinin of Influenza A Virus: Comparison of an Apathogenic Avian and a Mammalian Strain Pathogenic for Mink," *Virology* 165, no. 2 (1988): 428–437.
- [4] L. Englund and C. Hård af Segerstad, "Two Avian H10 Influenza A Virus Strains with Different Pathogenicity for Mink (Mustela vison)," *Archives of Virology* 143, no. 4 (1998): 653–666.
- [5] X. Lv, J. Tian, X. Li, et al., "H10Nx Avian Influenza Viruses Detected in Wild Birds in China Pose Potential Threat to Mammals," *One Health* 16 (2023): 100515.
- [6] G. G. Arzey, P. D. Kirkland, K. E. Arzey, et al., "Influenza Virus A (H10N7) in Chickens and Poultry Abattoir Workers, Australia," *Emerging Infectious Diseases* 18, no. 5 (2012): 814–816.
- [7] H. Chen, H. Yuan, R. Gao, et al., "Clinical and Epidemiological Characteristics of a Fatal Case of Avian Influenza A H10N8 Virus Infection: A Descriptive Study," *The Lancet* 383, no. 9918 (2014): 714–721.
- [8] W. Qi, X. Zhou, W. Shi, et al., "Genesis of the Novel Human-Infecting Influenza A(H10N8) Virus and Potential Genetic Diversity of the Virus in Poultry, China," *Eurosurveillance* 19, no. 25 (2014).
- [9] Q. Xian, Q. Haibo, H. Shixuan, et al., "Human Infection with an Avian-Origin Influenza A (H10N3) Virus," *New England Journal of Medicine* 386, no. 11 (2022): 1087–1088.
- [10] Q. Xu and F. Jiang, "CT of Human Infection with Avian-Origin Influenza A (H10N3) Virus," *Radiology* 304, no. 3 (2022): 531–531.
- [11] W. Zhang, Z. Zhang, M. Wang, X. Pan, and X. Jiang, "Second Identified Human Infection With the Avian Influenza Virus H10N3: A Case Report," *Annals of Internal Medicine* 176, no. 3 (2023): 429–431.
- [12] H. Jun, G. Lei, C. Xiaolong, et al., "A Retrospective Investigation of a Case of Dual Infection by Avian-Origin Influenza A (H10N5) and Seasonal Influenza A (H3N2) Viruses-2023-01," *China CDC Wkly* 6, no. 25 (2024).
- [13] C.-C. Lai and P.-R. Hsueh, "Human Infection Caused by Avian Influenza A (H10N5) Virus," *Journal of Microbiology, Immunology and Infection* 57, no. 3 (2024): 343–345.
- [14] K. Liu, X. Qi, C. Bao, X. Wang, and X. Liu, "Novel H10N3 Avian Influenza Viruses: A Potential Threat to Public Health," *The Lancet Microbe* 5, no. 5 (2024): e417.
- [15] D. S. Song, C. S. Lee, K. Jung, et al., "Isolation and Phylogenetic Analysis of H1N1 Swine Influenza Virus Isolated in Korea," *Virus Research* 125, no. 1 (2007): 98–103.
- [16] H. T. Chen, J. Zhang, D. H. Sun, et al., "Development of Reverse Transcription Loop-Mediated Isothermal Amplification for Rapid Detection of H9 Avian Influenza Virus," *Journal of Virological Methods* 151, no. 2 (2008): 200–203.
- [17] S. Payungporn, S. Chutinimitkul, A. Chaisingh, et al., "Single Step Multiplex Real-Time RT-PCR for H5N1 Influenza A Virus Detection," *Journal of Virological Methods* 131, no. 2 (2006): 143–147.
- [18] Z. Xie, Y. S. Pang, J. Liu, et al., "A Multiplex RT-PCR for Detection of Type A Influenza Virus and Differentiation of Avian H5, H7, and H9 Hemagglutinin Subtypes," *Molecular and Cellular Probes* 20, no. 3-4 (2006): 245–249.
- [19] H. T. Ho, H. L. Qian, F. He, et al., "Rapid Detection of H5N1 Subtype Influenza Viruses by Antigen Capture Enzyme-Linked Immunosorbent Assay Using H5- and N1-Specific Monoclonal Antibodies," *Clinical and Vaccine Immunology* 16, no. 5 (2009): 726–732.
- [20] C. Wang, X. Yang, S. Zheng, et al., "Development of an Ultrasensitive Fluorescent Immunochromatographic Assay Based on Multilayer Quantum Dot Nanobead for Simultaneous Detection of SARS-CoV-2 Antigen and Influenza A Virus," *Sens Actuators B Chem* 345 (2021): 130372.
- [21] D. Tseng, O. Mudanyali, C. Oztoprak, et al., "Lensfree Microscopy on a Cellphone," *Lab on a Chip* 10, no. 14 (2010): 1787–1792.
- [22] F. Wu, H. Yuan, C. Zhou, et al., "Multiplexed Detection of Influenza A Virus Subtype H5 and H9 via Quantum Dot-Based Immunoassay," *Biosensors and Bioelectronics* 77 (2016): 464–470.
- [23] X. Yu, L. Wei, H. Chen, et al., "Development of Colloidal Gold-Based Immunochromatographic Assay for Rapid Detection of Goose Parvovirus," *Frontiers in Microbiology* 9 (2018): 953.
- [24] Y. Zhao, G. Zhang, Q. Liu, M. Teng, J. Yang, and J. Wang, "Development of a Lateral Flow Colloidal Gold Immunoassay Strip for the Rapid Detection of Enrofloxacin Residues," *Journal of Agricultural and Food Chemistry* 56, no. 24 (2008): 12138–12142.
- [25] L. Sijie, D. Leina, Y. Xiaolin, et al., "Nanozyme Amplification Mediated on-Demand Multiplex Lateral Flow Immunoassay with Dual-Readout and Broadened Detection Range," *Biosensors and Bioelectronics* 169, no. 0 (2020): 112610.
- [26] S.-K. Kim, H. Sung, S.-H. Hwang, and M.-N. Kim, "A New Quantum Dot-Based Lateral Flow Immunoassay for the Rapid Detection of Influenza Viruses," *Biochip Journal* 16, no. 2 (2022): 175–182.
- [27] Z. Rong, Q. Wang, N. Sun, et al., "Smartphone-Based Fluorescent Lateral Flow Immunoassay Platform for Highly Sensitive Point-of-Care Detection of Zika Virus Nonstructural Protein 1," *Analytica Chimica Acta* 1055 (2019): 140–147.
- [28] Y. Shao, H. Duan, L. Guo, Y. Leng, W. Lai, and Y. Xiong, "Quantum Dot Nanobead-Based Multiplexed Immunochromatographic Assay for Simultaneous Detection of Aflatoxin B(1) and Zearalenone," *Analytica Chimica Acta* 1025 (2018): 163–171.

- [29] Z. Lu, Z. Zhu, X. Zheng, Y. Qiao, J. Guo, and C. M. Li, "Biocompatible Fluorescence-Enhanced ZrO<sub>2</sub>-CdTe Quantum Dot Nanocomposite For In Vitro Cell Imaging," *Nanotechnology* 22, no. 15 (2011): 155604.
- [30] A. V. T. Nguyen, T. D. Dao, T. T. T. Trinh, et al., "Sensitive Detection of Influenza A Virus Based on a CdSe/CdS/ZnS Quantum Dot-Linked Rapid Fluorescent Immunochromatographic Test," *Biosensors and Bioelectronics* 155 (2020): 112090.
- [31] O. Adegoke, M. Morita, T. Kato, M. Ito, T. Suzuki, and E. Y. Park, "Localized Surface Plasmon Resonance-Mediated Fluorescence Signals in Plasmonic Nanoparticle-Quantum Dot Hybrids for Ultrasensitive Zika Virus RNA Detection via Hairpin Hybridization Assays," *Biosensors and Bioelectronics* 94 (2017): 513–522.
- [32] J. Li, Y. Bai, F. Li, et al., "Rapid and Ultra-Sensitive Detection of African Swine Fever Virus Antibody on Site Using QDM Based-ASFV Immunosensor (QAIS)," *Analytica Chimica Acta* 1189 (2022): 339187.
- [33] X. Peng, F. Liu, H. Wu, et al., "Amino Acid Substitutions HA A150V, PA A343T, and PB2 E627K Increase the Virulence of H5N6 Influenza Virus in Mice," *Frontiers in Microbiology* 9 (2018): 453.
- [34] S. Chenguang, C. Junyu, L. Rui, et al., "A Multimechanistic Antibody Targeting the Receptor Binding Site Potentially Cross-Protects Against Influenza B Viruses," *Science Translational Medicine* 9, no. 412 (2017).
- [35] Y. Xiao, F. Yang, F. Liu, H. Yao, N. Wu, and H. Wu, "Antigen-Capture ELISA and Immunochromatographic Test Strip to Detect the H9N2 Subtype Avian Influenza Virus Rapidly Based on Monoclonal Antibodies," *Virology Journal* 18, no. 1 (2021): 198.
- [36] A. Nogales, M. S. Piepenbrink, J. Wang, et al., "A Highly Potent and Broadly Neutralizing H1 Influenza-Specific Human Monoclonal Antibody," *Scientific Reports* 8, no. 1 (2018): 4374.
- [37] K. A. Huang, P. Rijal, H. Jiang, et al., "Structure-Function Analysis of Neutralizing Antibodies to H7N9 Influenza from Naturally Infected Humans," *Nature Microbiology* 4, no. 2 (2019): 306–315.
- [38] Z. Sun, B. Shi, F. Meng, et al., "Development of a Colloidal Gold-Based Immunochromatographic Strip for Rapid Detection of H7N9 Influenza Viruses," *Frontiers in Microbiology* 9 (2018), 2069.
- [39] E. Hoffmann, J. Stech, Y. Guan, R. G. Webster, and D. R. Perez, "Universal Primer Set for the Full-Length Amplification of All Influenza A Viruses," *Archives of Virology* 146, no. 12 (2001): 2275–2289.
- [40] F. Yang, B. Chen, F. Liu, et al., "Development of a TaqMan MGB RT-PCR Assay for the Detection of Type A and Subtype H10 Avian Influenza Viruses," *Archives of Virology* 163, no. 9 (2018): 2497–2501.
- [41] F. Yang, Y. Xiao, B. Chen, et al., "Development of a Colloidal Gold-Based Immunochromatographic Strip Test Using Two Monoclonal Antibodies to Detect H7N9 Avian Influenza Virus," *Virus Genes* 56, no. 3 (2020): 396–400.
- [42] S. Zohari, A. Neimanis, T. Härkönen, C. Moraeus, and J. F. Valarcher, "Avian Influenza A(H10N7) Virus Involvement in Mass Mortality of Harbour Seals (*Phoca vitulina*) in Sweden, March Through October 2014," *Eurosurveillance* 19, no. 46 (2014).
- [43] Y. Xu, H. Cao, H. Liu, et al., "Identification of the Source of A (H10N8) Virus Causing Human Infection," *Infection, Genetics and Evolution* 30 (2015): 159–163.
- [44] M. Zhang, X. Zhang, K. Xu, et al., "Characterization of the Pathogenesis of H10N3, H10N7, and H10N8 Subtype Avian Influenza Viruses Circulating in Ducks," *Scientific Reports* 6, no. 1 (2016): 34489.
- [45] J. S. Krog, M. S. Hansen, E. Holm, et al., "Influenza A(H10N7) Virus in Dead Harbor Seals, Denmark," *Emerging Infectious Diseases* 21, no. 4 (2015): 684–687.
- [46] M. Liu, X. Li, H. Yuan, et al., "Genetic Diversity of Avian Influenza A (H10N8) Virus in Live Poultry Markets and Its Association With Human Infections in China," *Scientific Reports* 5, no. 1 (2015): 7632.
- [47] C. Su, S. Chen, X. Liu, et al., "Genome Sequence of a Novel H10N9 Avian Influenza Virus Isolated from Chickens in a Live Poultry Market in Eastern China," *Genome Announcements* 1, no. 4 (2013).
- [48] G. Deng, J. Shi, J. Wang, et al., "Genetics, Receptor Binding, and Virulence in Mice of H10N8 Influenza Viruses Isolated from Ducks and Chickens in Live Poultry Markets in China," *Journal of Virology* 89, no. 12 (2015): 6506–6510.
- [49] S. Ding, J. Zhou, J. Xiong, et al., "Continued Evolution of H10N3 Influenza Virus With Adaptive Mutations Poses an Increased Threat to Mammals," *Virologica Sinica* 39, no. 4 (2024): 546–555.
- [50] H. Fang, P. Mookkan, T. Yunrui, I. Kartigayen, K. Subaschandrabose Rajesh, and K. Jimmy, "Development of Dual-Function ELISA for Effective Antigen and Antibody Detection Against H7 Avian Influenza Virus," *BMC Microbiology* 13, no. 1 (2013).
- [51] X. Wen, Q. Xie, J. Li, et al., "Rapid and Sensitive Detection of African Swine Fever Virus in Pork Using Recombinase Aided Amplification Combined With QDMs-Based Test Strip," *Analytical and Bioanalytical Chemistry* 414, no. 13 (2022): 3885–3894.
- [52] E. K. Schneider, J. Li, and T. Velkov, "A Portrait of the Sialyl Glycan Receptor Specificity of the H10 Influenza Virus Hemagglutinin-A Picture of an Avian Virus on the Verge of Becoming a Pandemic?" *Vaccines* 5, no. 4 (2017): 51.
- [53] N. Tzarum, R. P. de Vries, W. Peng, et al., "The 150-Loop Restricts the Host Specificity of Human H10N8 Influenza Virus," *Cell Reports* 19, no. 2 (2017): 235–245.
- [54] J. Li, B. Liu, X. Tang, et al., "Development of a Smartphone-Based Quantum Dot Lateral Flow Immunoassay Strip for Ultrasensitive Detection of Anti-SARS-CoV-2 IgG and Neutralizing Antibodies," *International Journal of Infectious Diseases* 121 (2022): 58–65.
- [55] H. Wu, F. Yang, F. Liu, et al., "Molecular Characterization of H10 Subtype Avian Influenza Viruses Isolated From Poultry in Eastern China," *Archives of Virology* 164, no. 1 (2019): 159–179.